AF MIMO Relay Systems with Wireless Powered Relay Node and Direct Link

Bin Li and Yue Rong, *Senior Member, IEEE*

Abstract—A two-hop amplify-and-forward (AF) multiple-input multiple-output (MIMO) relay system with direct link is considered in this paper. The relay node has no self-power supply and relies on harvesting the radio frequency energy transferred from the source node to forward information from source to destination. In particular, we consider the time switching (TS) protocol between wireless information and energy transfer. We study the joint optimization of the source and relay precoding matrices and the TS factor to maximize the achievable source-destination rate when a single data stream is transmitted from the source node. The optimal structure of the source and relay precoding matrices is derived, which reduces the original problem to a simpler optimization problem. The simplified problem is then solved efficiently by a two-step method. Numerical simulations show that the proposed algorithm yields a higher rate and better rate-energy tradeoff than suboptimal approaches.

Index Terms—Amplify-and-forward, direct link, energy harvesting, MIMO relay, time switching receiver, wireless powered communication.

I. INTRODUCTION

A. Background

Recently, wireless energy transfer [1], [2] received increasing interests from both academia and industry due to the current proliferation of low power devices. Traditionally, wireless devices are powered by batteries with a limited life time. A high cost is usually associated with replacing batteries to extend the life time of wireless devices. Furthermore, due to physical and economic constraints, replacing batteries cannot be easily carried out in many scenarios in practice. For example, sometimes sensors may be embedded in building structures or even inside human bodies [3]. To avoid replacing batteries, some energy harvesting (EH) techniques were developed to power wireless networks with natural energy resources [4]-[6] such as solar and wind. However, due to the intermittent nature of these resources, they are hard to control and hence unreliable in real world applications. Compared with conventional EH techniques which rely on unstable natural resources, wireless energy transfer is a more promising and reliable technique, as radio frequency (RF) signals are used for EH which can be easily controlled. In addition, it

B. Li is with School of Electrical Engineering and Information, Sichuan University, Chengdu, China, e-mail: bin.li@scu.edu.cn.
Y. Rong is with the Department of Electrical and Computer Engineering, Curtin University, GPO Box U1987, Perth, WA 6845, Australia, e-mail: y.rong@curtin.edu.au.

provides great convenience to mobile users [7] by transferring information and energy with RF signals.

B. Literature Review

The receiver considered in [1] is capable of performing information decoding (ID) and EH simultaneously, and the trade-off between the achievable information rate and the harvested energy was characterized by a capacity-energy function. However, there are two challenges from practical considerations for the receiver proposed in [1]. Firstly, the circuits for harvesting energy cannot decode the carried information in practice [7]. To address this issue, a time switching (TS) protocol and a power splitting (PS) protocol were proposed in [8] to coordinate wireless information transfer (WIT) and wireless energy transfer (WET) at the receiver. Secondly, since WIT and WET operate with different sensitivity (-10dBm for energy receivers and -60dBm for information receivers), the architecture of the receiver in [1] may not be optimal for simultaneous wireless information and power transfer. To solve this problem, a separated architecture receiver and an integrated architecture receiver were developed in [7] for a more general protocol called dynamic power splitting which includes the TS protocol and the PS protocol as special cases.

Multiple-input multiple-output (MIMO) technique can improve the system energy and spectral efficiencies [9], [10]. By equipping multiple antennas at the access point, RF energy can be focused on wireless nodes so that they can be charged more efficiently compared with using a single antenna. Thus, the life time of energy constrained wireless networks can be extended. In [8], a MIMO broadcast channel with a separated architecture ID and EH receiver was investigated, where the energy-rate regions were derived for the TS protocol and the PS protocol. In [11], a multiple-input single-output (MISO) downlink system was considered, where the total transmission power was minimized by jointly optimizing the transmit beamforming vector and the PS ratio under a given signal-to-interference-plus-noise ratio (SINR).

Relay technology has been widely used to increase the coverage of wireless systems [12]-[16]. In a wireless powered communication (WPC) network, a relay node is able to harvest RF energy and receive information from the source node and then forwards the received information to the destination node using the harvested energy. The application of relays in WPC was addressed by some recent works [17]-[21]. In [17], TS and PS based relay protocols were proposed for a non-regenerative relay network. A full-duplex protocol was proposed in [18] for wireless-powered relay with self-energy

recycling. A wireless cooperative network was considered in [19] where multiple source-destination pairs communicate with each other via an EH relay node. The distribution of the harvested energy among multiple users and its impact on the system performance were studied in [19]. WPC with randomly located decode-and-forward (DF) relays was studied in [20], and it was shown that the use of EH relays can achieve the same diversity gain as conventional self-powered relays. In [21], a distributed PS framework based on game theory was developed for interference relay channels. It was shown in [22] that by using rateless codes, wireless-powered relay systems can achieve a higher rate than direct transmission without relaying.

The application of WPC in MIMO relay systems was studied in [2], [3], [23]-[26]. In [2], performance trade-offs of several receiver architectures were discussed by applying WPC in MIMO relay systems. Future research challenges in this area were also outlined in [2]. A TS protocol and a PS protocol were developed in [3] for a non-regenerative MIMO relay system, where the achievable rate was maximized for each protocol by jointly optimizing the source and relay precoding matrices. Precoder design for DF MIMO relay-based WPC networks was studied in [23] and [24]. In [25] and [26], an amplify-and-forward (AF) orthogonal space-time block code (OSTBC) based MIMO relay system with a multi-antenna EH receiver was investigated, where the source and relay precoding matrices were jointly optimized to achieve various tradeoffs between the energy transfer capability and the information rate.

C. Contributions

There are some recent works on transceiver optimization for self-powered MIMO relay systems, e.g. [12]-[16], [27], [28]. In [27], the optimal beamforming for DF relay channel was investigated. In [28], the optimal relay beamforming for two-way relay systems was been developed. However, the WPC technology was not applied in [27] and [28]. In [2] and [8], the concept of WPC was discussed and the structure of the optimal source precoding matrix for energy transfer was derived. However, the direct link was not considered in [2], and the relay technique was not applied in [8]. The direct link was considered in [23] and [24], but on DF-based MIMO relay networks. To the best of our knowledge, there is no work in the literature that studies the WPC in AF MIMO relay systems considering the direct source-destination link.

In this paper, we consider a two-hop AF MIMO relay system, where an EH receiver is equipped at the relay node to facilitate WPC. Different to existing works, we consider the direct link. One of the motivations of introducing a relay node when the direct link exists is to provide valuable spatial diversity to the channel between the source and destination nodes, which contributes to reduce the system bit-error-rate (BER). Moreover, through harvesting the radio frequency energy transferred from the source node, the relay node does not need to spend its own energy to forward information from source to destination. This helps to provide motivation for a selfish node to participate in the relay scheme.

The TS protocol is adopted during the source phase, where the source node transfers energy and information signals to the relay node during the first and second time intervals, respectively. During the second time interval, the source node also sends signal to the destination node through the direct link. Then, during the relay phase, the relay node uses the harvested energy to forward the received information to the destination node. To extend the life time of the network, an energy constraint is used in this paper so that the energy consumed for relaying signals from the relay node to the destination is only obtained from the source node via EH.

The joint optimization of the source and relay precoding matrices and the TS factor is investigated to maximize the achievable source-destination rate when a single data stream is transmitted from the source node, subjecting to the harvested energy constraint at the relay node and the energy constraint at the source node. The optimal structure of the source and relay precoding matrices is derived, which reduces the original problem to a simpler optimization problem. Interestingly, we show that the optimal source precoding vector for the information transfer has a generalized beamforming structure. Based on the observation that the achievable system rate is a unimodal function of the TS factor, a two-step method is developed to efficiently solve the simplified problem. In the first step, the TS factor is optimized by the golden section search method. The subproblem with a fixed TS factor is then solved through solving two nonlinear equations in the second step. To limit the power of energy transfer at the source node, a practical peak power constraint is considered. A two-step approach is proposed by checking the activeness of this constraint. Numerical simulations show that the proposed algorithm yields a higher rate and better rate-energy tradeoff than suboptimal approaches. Interestingly, the rate achieved by systems with peak power constraint approaches that of the system with energy constraint when the value of the peak power is high.

The contributions of this paper are summarized as follows: (1) The direct link between the source and destination nodes is considered in WPC based MIMO relay systems; (2) An energy constraint at the source node is proposed, which is more general than existing constant power constraints based formulation; (3) The optimal structure of the source and relay precoding matrices under the energy constraint is derived; (4) A two-step approach is developed for solving the transceiver optimization problem; (5) A peak power constraint is considered and the corresponding solution scheme is developed. The relationships between the power constraint based design and the energy constraint based design are discussed.

D. Structure

The rest of the paper is organized as follows. The model of a two-hop AF MIMO relay system with direct link utilizing WPC is presented in Section II. In this section, the transceiver optimization problem is also formulated. The proposed algorithms are developed in Section III. Numerical examples are presented in Section IV to demonstrate the performance of the proposed algorithms. Finally, we conclude our paper in Section V.
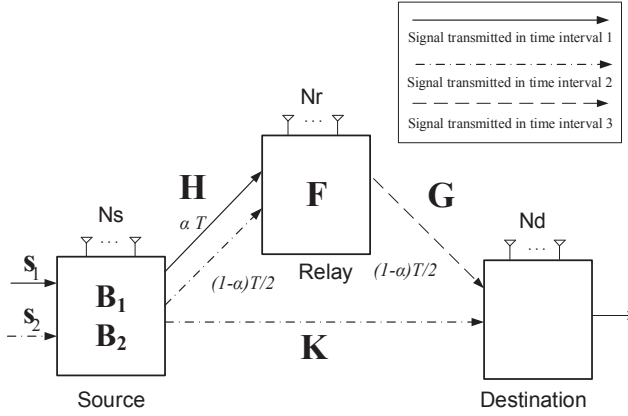
Fig. 1. A two-hop MIMO relay communication system with direct link and an energy-harvesting relay node.

II. SYSTEM MODEL

We consider a three-node two-hop MIMO communication system where the source node S transmits information to the destination node D with the aid of one relay node R as shown in Fig. 1. The source, relay, and destination nodes are equipped with N_s, N_r, and N_d antennas, respectively. We assume that the source node has its own power supply, while the relay node is powered by harvesting the RF energy sent from the source node.

In this paper, the WPC technology is applied for energy harvesting and information transmission. In particular, a time switching protocol [8] is considered. With this protocol, there are three intervals in one communication cycle T. In the first time interval, energy is transferred from the source node to the relay node with a duration of αT, where $0 < \alpha < 1$ denotes the time switching factor. In the second time interval, information signals are transmitted from the source node to the relay node with a duration of $(1 - \alpha)T/2$. Meanwhile, these signals are also transmitted to the destination node via the direct link. The last time interval of $(1-\alpha)T/2$ is used for relaying the information signals received by the relay node to the destination node. For the simplicity of presentation, we set $T = 1$ hereafter. In all three time intervals, signals are linearly precoded before transmission.

More specifically, in the first time interval, an $N_1 \times 1$ energy-carrying signal vector $\mathbf{s}_1$ is precoded by an $N_s \times N_1$ matrix $\mathbf{B}_1$ at the source node and transmitted to the relay node. The optimal value of N_1 will be determined later. We assume that $E\{\mathbf{s}_1\mathbf{s}_1^H\} = \mathbf{I}_{N_1}$, where $E\{\cdot\}$ stands for the statistical expectation, $\mathbf{I}_n$ is an $n \times n$ identity matrix, and $(\cdot)^H$ denotes the Hermitian transpose. The received signal vector at the relay node is given by

$$\mathbf{y}_{r,1} = \mathbf{H}\mathbf{B}_1\mathbf{s}_1 + \mathbf{v}_{r,1} \tag{1}$$

where $\mathbf{H}$ is an $N_r \times N_s$ MIMO channel matrix between the source and relay nodes, $\mathbf{y}_{r,1}$ and $\mathbf{v}_{r,1}$ are the received signal and the noise vectors at the relay node during the first interval,

respectively. Based on the linear energy harvesting model [3], [8], [17]-[26], the RF energy harvested at the relay node is proportional to the baseband received signal in (1) without the noise component, which is given by

$$\bar{E}_r = \xi_1 \alpha \mathrm{tr}(\mathbf{H}\mathbf{B}_1\mathbf{B}_1^H\mathbf{H}^H)$$

where $\mathrm{tr}(\cdot)$ denotes the matrix trace and $0 < \xi_1 \leq 1$ is the energy conversion efficiency[1]. Moreover, considering the energy loss in practical communication systems due to the signal processing operations, the energy available at the relay node to forward the received signals is given by

$$E_r = \xi_2\bar{E}_r = \xi\alpha\mathrm{tr}(\mathbf{H}\mathbf{B}_1\mathbf{B}_1^H\mathbf{H}^H) \tag{2}$$

where $0 < \xi_2 \leq 1$, $\xi = \xi_1\xi_2$, and $(1 - \xi_2)\bar{E}_r$ models the energy loss in practical systems.

During the second time interval, an information-bearing signal s_2 with $E\{|s_2|^2\} = 1$ is precoded by an $N_s \times 1$ vector $\mathbf{b}_2$ at the source node and transmitted to the relay node. The received signal vector at the relay node can be written as

$$\mathbf{y}_{r,2} = \mathbf{H}\mathbf{b}_2 s_2 + \mathbf{v}_{r,2} \tag{3}$$

where $\mathbf{v}_{r,2}$ is the noise vector at the relay node during the second interval. While the received signal vector at the destination node in this time interval can be written as

$$\mathbf{y}_{d,2} = \mathbf{K}\mathbf{b}_2 s_2 + \mathbf{v}_{d,2} \tag{4}$$

where $\mathbf{K}$ is an $N_d \times N_s$ channel matrix between the source and destination nodes, $\mathbf{y}_{d,2}$ and $\mathbf{v}_{d,2}$ are the received signal and noise vectors at the destination node in the second time interval, respectively.

Finally, during the third time interval, the relay node linearly precodes $\mathbf{y}_{r,2}$ with an $N_r \times N_r$ matrix $\mathbf{F}$ and transmits the precoded signal vector

$$\mathbf{x}_r = \mathbf{F}\mathbf{y}_{r,2} \tag{5}$$

to the destination node. From (3) and (5), the received signal vector at the destination node in the third time interval can be written as

$$\begin{aligned}\mathbf{y}_{d,3} &= \mathbf{G}\mathbf{x}_r + \mathbf{v}_{d,3} \\ &= \mathbf{G}\mathbf{F}\mathbf{H}\mathbf{b}_2 s_2 + \mathbf{G}\mathbf{F}\mathbf{v}_{r,2} + \mathbf{v}_{d,3}\end{aligned} \tag{6}$$

where $\mathbf{G}$ is an $N_d \times N_r$ MIMO channel matrix between the relay and destination nodes, $\mathbf{y}_{d,3}$ and $\mathbf{v}_{d,3}$ are the received signal and noise vectors at the destination node in the third time interval, respectively.

Combining (4) and (6), the received signal vector at the destination node over the second and the third time intervals is given by

$$\mathbf{y} \triangleq \begin{bmatrix}\mathbf{y}_{d,3} \\ \mathbf{y}_{d,2}\end{bmatrix} = \begin{bmatrix}\mathbf{G}\mathbf{F}\mathbf{H} \\ \mathbf{K}\end{bmatrix}\mathbf{b}_2 s_2 + \begin{bmatrix}\mathbf{G}\mathbf{F}\mathbf{v}_{r,2} + \mathbf{v}_{d,3} \\ \mathbf{v}_{d,2}\end{bmatrix}. \tag{7}$$

We assume that $\mathbf{H}$, $\mathbf{G}$, and $\mathbf{K}$ are quasi-static and known at the relay node. All noises are assumed to be additive white Gaussian noise (AWGN) with zero-mean, $E\{\mathbf{v}_{r,2}\mathbf{v}_{r,2}^H\} = \sigma_r^2\mathbf{I}_{N_r}$,

---

[1]Extending the results in this paper to systems with nonlinear energy harvesting models [29]-[32] is an interesting and challenging future topic.

and $E\{\mathbf{v}_{d,2}\mathbf{v}_{d,2}^H\} = E\{\mathbf{v}_{d,3}\mathbf{v}_{d,3}^H\} = \sigma_d^2\mathbf{I}_{N_d}$. We also assume that s_2 has Gaussian distribution.

From (7), the achievable rate from the source node to the destination node can be written as [13]

$$
\begin{aligned}
&\mathrm{R}(\alpha, \mathbf{b}_2, \mathbf{F}) \\
&= \frac{1-\alpha}{2}\log_2(1+\sigma_d^{-2}\mathbf{b}_2^H\mathbf{K}^H\mathbf{K}\mathbf{b}_2+\mathbf{b}_2^H\mathbf{H}^H\mathbf{F}^H\mathbf{G}^H \\
&\quad \times(\sigma_r^2\mathbf{G}\mathbf{F}\mathbf{F}^H\mathbf{G}^H + \sigma_d^2\mathbf{I}_{N_d})^{-1}\mathbf{G}\mathbf{F}\mathbf{H}\mathbf{b}_2)
\end{aligned} \tag{8}
$$

where $(\cdot)^{-1}$ denotes the matrix inversion. Note that the energy used to transmit $\mathbf{s}_1$ and s_2 from the source node is $\alpha\mathrm{tr}(\mathbf{B}_1\mathbf{B}_1^H)$ and $\frac{1-\alpha}{2}\mathbf{b}_2^H\mathbf{b}_2$, respectively. Therefore, the constraint on the energy consumed by the source node can be written as

$$
\alpha\mathrm{tr}(\mathbf{B}_1\mathbf{B}_1^H) + \frac{1-\alpha}{2}\mathbf{b}_2^H\mathbf{b}_2 \le \frac{1+\alpha}{2}P_s \tag{9}
$$

where P_s is the nominal (average) power available at the source node. Note that the energy constraint (9) is more relaxed than the constant power constraints

$$
\mathrm{tr}(\mathbf{B}_1\mathbf{B}_1^H) \le P_s, \quad \mathbf{b}_2^H\mathbf{b}_2 \le P_s \tag{10}
$$

in existing works (e.g. [3]), since if (10) is satisfied, then (9) also holds. In this sense, (9) is more general and includes (10) as a special case.

From (3) and (5), the energy consumed by the relay node to transmit $\mathbf{x}_r$ to the destination node is given by

$$
\frac{1-\alpha}{2}\mathrm{tr}(E\{\mathbf{x}_r\mathbf{x}_r^H\}) = \frac{1-\alpha}{2}\mathrm{tr}(\mathbf{F}(\mathbf{H}\mathbf{b}_2\mathbf{b}_2^H\mathbf{H}^H+\sigma_r^2\mathbf{I}_{N_r})\mathbf{F}^H). \tag{11}
$$

Based on (2) and (11), we obtain the following energy constraint at the relay node

$$
\frac{1-\alpha}{2}\mathrm{tr}(\mathbf{F}(\mathbf{H}\mathbf{b}_2\mathbf{b}_2^H\mathbf{H}^H+\sigma_r^2\mathbf{I}_{N_r})\mathbf{F}^H) \le \alpha\xi\mathrm{tr}(\mathbf{H}\mathbf{B}_1\mathbf{B}_1^H\mathbf{H}^H). \tag{12}
$$

With only the energy constraint (9), the transmission power at the source node at the first time interval might increase to a large value when α approaches 0. This is more likely to occur at large P_s. To impose constraint on the peak transmission power, we introduce

$$
\mathrm{tr}(\mathbf{B}_1\mathbf{B}_1^H) \le P_m. \tag{13}
$$

From (8), (9), (12), and (13), the transceiver optimization problem for linear AF wireless information and energy transfer MIMO relay systems can be written as[2]

$$
\max_{0<\alpha<1,\mathbf{B}_1,\mathbf{b}_2,\mathbf{F}} \mathrm{R}(\alpha, \mathbf{b}_2, \mathbf{F}) \tag{14}
$$

$$
\text{s.t. } \alpha\mathrm{tr}(\mathbf{B}_1\mathbf{B}_1^H) + \frac{1-\alpha}{2}\mathbf{b}_2^H\mathbf{b}_2 \le \frac{1+\alpha}{2}P_s \tag{15}
$$

$$
\mathrm{tr}(\mathbf{F}(\mathbf{H}\mathbf{b}_2\mathbf{b}_2^H\mathbf{H}^H+\sigma_r^2\mathbf{I}_{N_r})\mathbf{F}^H) \le \frac{2\alpha\xi}{1-\alpha}\mathrm{tr}(\mathbf{H}\mathbf{B}_1\mathbf{B}_1^H\mathbf{H}^H) \tag{16}
$$

$$
\mathrm{tr}(\mathbf{B}_1\mathbf{B}_1^H) \le P_m. \tag{17}
$$

[2]It is not easy to generalize the approaches in this paper to the multiple data streams case. One of the challenges is that as shown in [13] and [14], even for self-powered relay node, it is not easy to optimize the relay precoding matrix $\mathbf{F}$ with multiple data streams (no closed-form optimal solution) when the direct link is considered.

III. THE PROPOSED ALGORITHM

The problem (14)-(17) is nonconvex with matrix variables and is challenging to solve. In this section, we develop a novel algorithm to solve the problem (14)-(17). We first study the case that (17) is inactive at the optimal solution, then the problem (14)-(17) is reduced to the following problem

$$
\max_{0<\alpha<1,\mathbf{B}_1,\mathbf{b}_2,\mathbf{F}} \mathrm{R}(\alpha, \mathbf{b}_2, \mathbf{F}) \tag{18}
$$

$$
\text{s.t. } \alpha\mathrm{tr}(\mathbf{B}_1\mathbf{B}_1^H) + \frac{1-\alpha}{2}\mathbf{b}_2^H\mathbf{b}_2 \le \frac{1+\alpha}{2}P_s \tag{19}
$$

$$
\mathrm{tr}(\mathbf{F}(\mathbf{H}\mathbf{b}_2\mathbf{b}_2^H\mathbf{H}^H+\sigma_r^2\mathbf{I}_{N_r})\mathbf{F}^H) \le \frac{2\alpha\xi}{1-\alpha}\mathrm{tr}(\mathbf{H}\mathbf{B}_1\mathbf{B}_1^H\mathbf{H}^H). \tag{20}
$$

The impact of the constraint (17) will be studied later.

A. The Optimal Structure of $\mathbf{B}_1$ and $\mathbf{F}$

First, we derive the optimal structure of $\mathbf{B}_1$ and $\mathbf{F}$, under which the problem (18)-(20) can be simplified. Let us introduce

$$
\mathbf{H} = \mathbf{U}_h\mathbf{\Lambda}_h^{\frac{1}{2}}\mathbf{V}_h^H, \quad \mathbf{G} = \mathbf{U}_g\mathbf{\Lambda}_g^{\frac{1}{2}}\mathbf{V}_g^H \tag{21}
$$

as the singular value decompositions (SVDs) of $\mathbf{H}$ and $\mathbf{G}$, respectively, with the diagonal elements of $\mathbf{\Lambda}_h$ and $\mathbf{\Lambda}_g$ sorted in decreasing order.

THEOREM 1: The optimal $\mathbf{B}_1$ and $\mathbf{F}$ as the solution to the problem (18)-(20) has the following structure

$$
\mathbf{B}_1^* = \lambda_b^{\frac{1}{2}}\mathbf{v}_{h,1}, \quad \mathbf{F}^* = c^{\frac{1}{2}}\mathbf{v}_{g,1}\mathbf{b}_2^H\mathbf{H}^H \tag{22}
$$

where $(\cdot)^*$ stands for the optimal value, λ_b and c are positive scalars that remain to be optimized, $\mathbf{v}_{h,1}$ and $\mathbf{v}_{g,1}$ are the first columns of $\mathbf{V}_h$ and $\mathbf{V}_g$, respectively.

PROOF: See Appendix A. $\square$

It is interesting to see from (22) that the optimal $\mathbf{B}_1$ is a vector (i.e., $N_1 = 1$) matching $\mathbf{v}_{h,1}$. This indicates that in order to maximize the energy harvested by the relay node, all transmission power at the source node should be allocated to the channel corresponding to the largest singular value of $\mathbf{H}$ during the first time interval. As a result, we only need to optimize λ_b in $\mathbf{B}_1$. It can also be seen from (22) that the optimal structure of $\mathbf{F}$ is similar to that in two-hop MIMO relay systems where the relay node has self-power supply [13].

Based on Theorem 1, the matrix optimization problem (18)-(20) can be reduced to a simpler problem. This can be done by substituting (22) back into (18)-(20), and we have

$$
\max_{\alpha,\mathbf{b}_2,c,\lambda_b} \frac{1-\alpha}{2}\log_2\left(1+\frac{\|\mathbf{K}\mathbf{b}_2\|^2}{\sigma_d^2}+\frac{c\lambda_{g,1}\|\mathbf{H}\mathbf{b}_2\|^4}{\sigma_d^2+\sigma_r^2c\lambda_{g,1}\|\mathbf{H}\mathbf{b}_2\|^2}\right) \tag{23}
$$

$$
\text{s.t. } \alpha\lambda_b + \frac{1-\alpha}{2}\|\mathbf{b}_2\|^2 \le \frac{1+\alpha}{2}P_s \tag{24}
$$

$$
c(\|\mathbf{H}\mathbf{b}_2\|^4 + \sigma_r^2\|\mathbf{H}\mathbf{b}_2\|^2) \le \frac{2\alpha\xi}{1-\alpha}\lambda_{h,1}\lambda_b \tag{25}
$$

where $\|\cdot\|$ stands for the vector Euclidian norm and $\lambda_{h,1}$ denotes the first diagonal element of $\mathbf{\Lambda}_h$. As (23) monotonically increases with $\|\mathbf{H}\mathbf{b}_2\|^2$, for any λ_b, the optimal $\mathbf{b}_2$ maximizing (23) must satisfy equality in the constraint (25), i.e.,

$$
\alpha\lambda_b = \frac{(1-\alpha)c}{2\xi\lambda_{h,1}}(\|\mathbf{H}\mathbf{b}_2\|^4 + \sigma_r^2\|\mathbf{H}\mathbf{b}_2\|^2). \tag{26}
$$

By substituting (26) back into (24), the problem (23)-(25) can be equivalently rewritten as

$$\max_{\alpha,\mathbf{b}_2,c} \frac{1-\alpha}{2}\log_2\left(1+\frac{\|\mathbf{Kb}_2\|^2}{\sigma_d^2}+\frac{c\lambda_{g,1}\|\mathbf{Hb}_2\|^4}{\sigma_d^2+\sigma_r^2c\lambda_{g,1}\|\mathbf{Hb}_2\|^2}\right) \quad (27)$$

$$\text{s.t.} \ \frac{c}{\xi\lambda_{h,1}}(\|\mathbf{Hb}_2\|^4+\sigma_r^2\|\mathbf{Hb}_2\|^2)+\|\mathbf{b}_2\|^2 \leq P_s\frac{1+\alpha}{1-\alpha}. \quad (28)$$

To proceed further, we define $M(\alpha)$ as the optimal value of the following problem for a given α

$$\max_{\mathbf{b}_2,c} \log_2\left(1+\frac{\|\mathbf{Kb}_2\|^2}{\sigma_d^2}+\frac{c\lambda_{g,1}\|\mathbf{Hb}_2\|^4}{\sigma_d^2+\sigma_r^2c\lambda_{g,1}\|\mathbf{Hb}_2\|^2}\right) \quad (29)$$

$$\text{s.t.} \ \frac{c}{\xi\lambda_{h,1}}(\|\mathbf{Hb}_2\|^4+\sigma_r^2\|\mathbf{Hb}_2\|^2)+\|\mathbf{b}_2\|^2 \leq P_\alpha \quad (30)$$

where $P_\alpha = P_s\frac{1+\alpha}{1-\alpha}$. Then, the optimal value of the problem (27)-(28) can be written as

$$F(\alpha) = \frac{1-\alpha}{2}M(\alpha). \quad (31)$$

The unimodality of $F(\alpha)$ is difficult to prove rigorously[3], and it will be illustrated graphically later in this section. Based on this observation, the problem (27)-(28) can be efficiently solved by a two-step algorithm, where for a given α we optimize $\mathbf{b}_2$ and c by solving the problem (29)-(30). And then a simple one dimensional search (such as the golden section search method [33]) can be applied to obtain the optimal α. The procedure of the proposed two-step algorithm is summarized in Algorithm 1, where ε is a positive constant close to 0, and $\delta > 0$ is the reduction factor. It is shown in [33] that the optimal $\delta = 1.618$, also known as the golden ratio. Finally, the optimal precoding matrices are obtained as Step 12 in Algorithm 1.

B. Solving the Problem (29)-(30)

As (29) monotonically increases with c, for any $\|\mathbf{b}_2\|^2 \leq P_\alpha$, the optimal c maximizing (29) must satisfy equality in (30), i.e.,

$$c\|\mathbf{Hb}_2\|^2 = \frac{\xi\lambda_{h,1}(P_\alpha-\|\mathbf{b}_2\|^2)}{\|\mathbf{Hb}_2\|^2+\sigma_r^2}. \quad (32)$$

Substituting (32) back into (29), we have

$$\log_2\left(1+\frac{\|\mathbf{Kb}_2\|^2}{\sigma_d^2}+\frac{c\lambda_{g,1}\|\mathbf{Hb}_2\|^4}{\sigma_d^2+\sigma_r^2c\lambda_{g,1}\|\mathbf{Hb}_2\|^2}\right)$$

$$=\log_2\left(1+\frac{\|\mathbf{Kb}_2\|^2}{\sigma_d^2}+\frac{\bar{\lambda}(P_\alpha-\|\mathbf{b}_2\|^2)\|\mathbf{Hb}_2\|^2}{\sigma_d^2(\|\mathbf{Hb}_2\|^2+\sigma_r^2)+\sigma_r^2\bar{\lambda}(P_\alpha-\|\mathbf{b}_2\|^2)}\right)$$

$$=\log_2\left(1+\frac{1}{\sigma_d^2}\left(\|\mathbf{Kb}_2\|^2\right.\right.$$

$$\left.\left.+\frac{\sigma_d^2\lambda(P_\alpha-\|\mathbf{b}_2\|^2)\|\mathbf{Hb}_2\|^2}{(\|\mathbf{Hb}_2\|^2+\sigma_r^2)+\sigma_r^2\lambda(P_\alpha-\|\mathbf{b}_2\|^2)}\right)\right) \quad (33)$$

[3]The difficulty is that α changes the value of $M(\alpha)$ through varying the feasible region of the optimization problem (29)-(30), and the objective function (29) is a complicated function. As a result, the closed-form expression of $M(\alpha)$ is difficult to obtain.

Algorithm 1 Procedure of Applying the Golden Section Search to Find the Optimal α and the Precoding Matrices.

Input: P_s, $\lambda_{g,1}$, σ_r^2, σ_d^2, $\mathbf{H}$, and $\mathbf{K}$.
Output: α^*, $\mathbf{B}_1^*$, and $\mathbf{F}^*$.
 Initialization: $\alpha_l = 0$ and $\alpha_u = 1$.
1: **while** $|\alpha_u - \alpha_l| > \varepsilon$ **do**
2:    Define $d_1 = (\delta-1)\alpha_l+(2-\delta)\alpha_u$ and $d_2 = (2-\delta)\alpha_l+(\delta-1)\alpha_u$.
3:    Solve the problem (29)-(30) for $\alpha = d_1$; Compute $F(d_1)$ for $\alpha = d_1$.
4:    Repeat Step 3 for $\alpha = d_2$.
5:    **if** $F(d_1) < F(d_2)$ **then**
6:      Assign $\alpha_l = d_1$.
7:    **else**
8:      Assign $\alpha_u = d_2$.
9:    **end if**
10: **end while**
11: $\alpha^* = (\alpha_u + \alpha_l)/2$.
12: Calculate the optimal $\mathbf{B}_1^*$ and $\mathbf{F}^*$ based on (22) where

$$\lambda_b^* = \frac{(1-\alpha^*)c^*}{2\alpha^*\xi\lambda_{h,1}}\left(\|\mathbf{Hb}_2^*\|^4+\sigma_r^2\|\mathbf{Hb}_2^*\|^2\right).$$

where $\bar{\lambda} = \xi\lambda_{h,1}\lambda_{g,1}$ and $\lambda = \xi\lambda_{h,1}\lambda_{g,1}/\sigma_d^2$. Using (33), the problem (29)-(30) can be equivalently written as

$$\max_{\|\mathbf{b}_2\|^2\leq P_\alpha} \|\mathbf{Kb}_2\|^2+\frac{\sigma_d^2\lambda(P_\alpha-\|\mathbf{b}_2\|^2)\|\mathbf{Hb}_2\|^2}{(\|\mathbf{Hb}_2\|^2+\sigma_r^2)+\sigma_r^2\lambda(P_\alpha-\|\mathbf{b}_2\|^2)}. \quad (34)$$

By introducing new variables x and y with $\lambda(P_\alpha-\|\mathbf{b}_2\|^2) \geq x$ and $\|\mathbf{Hb}_2\|^2 \geq y$, the problem (34) can be converted to

$$\max_{x,y,\mathbf{b}_2} \|\mathbf{Kb}_2\|^2+\frac{\sigma_d^2xy}{\sigma_r^2x+y+\sigma_r^2} \quad (35)$$

$$\text{s.t.} \ \|\mathbf{Hb}_2\|^2 \geq y \quad (36)$$

$$\|\mathbf{b}_2\|^2 \leq P_\alpha - x/\lambda. \quad (37)$$

PROPOSITION 1: The problem (35)-(37) admits strong duality.

PROOF: See Appendix B. □

The problem (35)-(37) can be solved by the Lagrange multiplier method. The corresponding Lagrangian function is given by

$$L = -\|\mathbf{Kb}_2\|^2 - \frac{\sigma_d^2xy}{\sigma_r^2x+y+\sigma_r^2} + \beta(y-\|\mathbf{Hb}_2\|^2)$$

$$+\gamma(\|\mathbf{b}_2\|^2 - P_\alpha + x/\lambda) \quad (38)$$

where $\beta \geq 0$ and $\gamma \geq 0$ are the Lagrange multipliers. Based on the Karush-Kuhn-Tucker (KKT) optimality conditions, we obtain from (38) that

$$\frac{\partial L}{\partial \mathbf{b}_2} = -\mathbf{b}_2^H\mathbf{K}^H\mathbf{K} - \beta\mathbf{b}_2^H\mathbf{H}^H\mathbf{H} + \gamma\mathbf{b}_2^H = 0 \quad (39)$$

$$\frac{\partial L}{\partial x} = -\frac{\sigma_d^2y(y+\sigma_r^2)}{(\sigma_r^2x+y+\sigma_r^2)^2} + \frac{\gamma}{\lambda} = 0 \quad (40)$$

$$\frac{\partial L}{\partial y} = -\frac{\sigma_r^2\sigma_d^2x(x+1)}{(\sigma_r^2x+y+\sigma_r^2)^2} + \beta = 0. \quad (41)$$

From (39), we have

$$(\beta\mathbf{H}^H\mathbf{H} + \mathbf{K}^H\mathbf{K})\mathbf{b}_2 = \gamma\mathbf{b}_2. \qquad (42)$$

From (42), we can obtain the following proposition on the optimal structure of $\mathbf{b}_2$.

PROPOSITION 2: The optimal $\mathbf{b}_2$ has the following structure

$$\mathbf{b}_2^* = \sqrt{\eta^*}\mathbf{v}(\beta^*\mathbf{H}^H\mathbf{H} + \mathbf{K}^H\mathbf{K}) \qquad (43)$$

where η^* is a positive scalar, $\mathbf{v}(\mathbf{A})$ stands for the principal eigenvector of matrix $\mathbf{A}$ with $\|\mathbf{v}(\mathbf{A})\| = 1$.

REMARK 1: It is interesting to see from (43) that the optimal $\mathbf{b}_2$ has a generalized beamforming structure, which has a strong connection to its physical meaning in practice. Note that $\mathbf{b}_2$ is the precoding vector used for transmitting information from the source node to the relay node through $\mathbf{H}$ and from the source node to the destination node through $\mathbf{K}$. In (43), the optimal $\mathbf{b}_2$ is determined by the principal eigenvector of $\beta^*\mathbf{H}^H\mathbf{H} + \mathbf{K}^H\mathbf{K}$, which is a linear combination of $\mathbf{H}^H\mathbf{H}$ and $\mathbf{K}^H\mathbf{K}$. Here, β^* can be regarded as the optimal weight factor. To find $\mathbf{b}_2$, its magnitude $\sqrt{\eta^*}$ and β^* need to be properly chosen. This can be achieved by solving two nonlinear equations as shown later in this section.

For the simplicity of notations, we denote $\mathbf{b}_2^* = \sqrt{\eta^*}\mathbf{v}(\beta^*)$. From (42), the optimal γ is $\gamma^* = e(\beta^*\mathbf{H}^H\mathbf{H} + \mathbf{K}^H\mathbf{K})$, where $e(\mathbf{A})$ stands for the principal eigenvalue of matrix $\mathbf{A}$. Similarly, we denote $\gamma^* = e(\beta^*)$ for the simplicity of notation.

As (35) monotonically increases with $x > 0$ and $y > 0$, to maximize (35), equalities in (36) and (37) must hold at the optimal solution. Therefore, we have

$$y^* = \eta^*\|\mathbf{H}\mathbf{v}(\beta^*)\|^2, \qquad x^* = \lambda(P_\alpha - \eta^*). \qquad (44)$$

The rest of the problem is to find β^* and η^*. This can be done by substituting (44) back into (40) and (41) and solving the following system of two nonlinear equations

$$\beta^* = \frac{\sigma_r^2\sigma_d^2\lambda(P_\alpha - \eta^*)(\lambda(P_\alpha - \eta^*) + 1)}{(\sigma_r^2\lambda(P_\alpha - \eta^*) + \eta^*\|\mathbf{H}\mathbf{v}(\beta^*)\|^2 + \sigma_r^2)^2} \qquad (45)$$

$$\frac{e(\beta^*)}{\lambda} = \frac{\sigma_d^2\eta^*\|\mathbf{H}\mathbf{v}(\beta^*)\|^2(\eta^*\|\mathbf{H}\mathbf{v}(\beta^*)\|^2 + \sigma_r^2)}{(\sigma_r^2\lambda(P_\alpha - \eta^*) + \eta^*\|\mathbf{H}\mathbf{v}(\beta^*)\|^2 + \sigma_r^2)^2}. \qquad (46)$$

As (45)-(46) are two-dimensional nonlinear equations of β^* and η^*, they can be efficiently solved by using standard software packages via, for example, the Newton's method, the Broyden's method (quasi-Newton method), and the gradient method [33].

Let us denote

$f_1(\beta, \eta) = \beta\Delta(\beta, \eta) - \sigma_r^2\sigma_d^2\lambda(P_\alpha - \eta)(\lambda(P_\alpha - \eta) + 1)$

$f_2(\beta, \eta) = e(\beta)\Delta(\beta, \eta) - \sigma_d^2\lambda\eta\|\mathbf{H}\mathbf{v}(\beta)\|^2(\eta\|\mathbf{H}\mathbf{v}(\beta)\|^2 + \sigma_r^2)$

where

$$\Delta(\beta, \eta) = (\sigma_r^2\lambda(P_\alpha - \eta) + \eta\|\mathbf{H}\mathbf{v}(\beta)\|^2 + \sigma_r^2)^2.$$

Then nonlinear equations (45)-(46) can be rewritten as

$$\begin{bmatrix} f_1(\beta, \eta) \\ f_2(\beta, \eta) \end{bmatrix} = \begin{bmatrix} 0 \\ 0 \end{bmatrix}. \qquad (47)$$

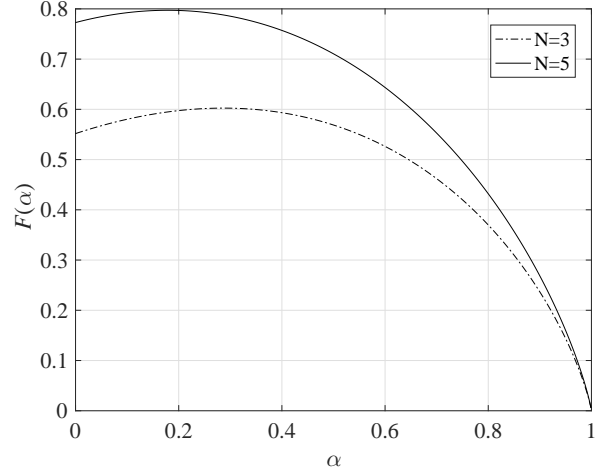To solve (47), we derive the Jacobian matrix of (47) in Appendix C.

Fig. 2. Unimodality of $F(\alpha)$, $P_s = 5$dBm.

Based on the discussions above, we develop an efficient algorithm to solve the problem (29)-(30) as summarized in Algorithm 2. Firstly, for a given α, we solve (45) and (46) to obtain β^* and η^*. Then, we compute $\mathbf{b}_2^*$ through (43). Finally, c^* is obtained from (32).

Algorithm 2 Procedure of Solving the Problem (29)-(30).

Input: α, P_s, λ, σ_r^2, σ_d^2, $\mathbf{H}$, and $\mathbf{K}$.
Output: $\mathbf{b}_2^*$ and c^*.
 1: Solve (45) and (46) for the optimal β^* and η^*.
 2: Compute $\mathbf{b}_2^*$ according to (43).
 3: Calculate c^* based on (32).

To verify the unimodality of $F(\alpha)$ in (31), we solve the problem (27)-(28) using the method proposed in Algorithm 1 and Algorithm 2 to calculate $F(\alpha)$ numerically. We set $P_s = 5$dBm, $\sigma_r^2 = \sigma_d^2 = -50$dBm, and $N_s = N_r = N_d = N$. Fig. 2 shows $F(\alpha)$ versus α with $N = 3$ and $N = 5$, respectively, calculated by using the proposed algorithm described above. It can be seen that $F(\alpha)$ indeed is a unimodal function of α.

C. Peak Power Constraint

In this section, we consider the peak power constraint (17). Based on Theorem 1, (17) can be rewritten as

$$\lambda_b \leq P_m. \qquad (48)$$

By including (48) in the problem (23)-(25), we obtain the following problem for a given α

$$\max_{\mathbf{b}_2,c,\lambda_b} \log_2\left(1 + \frac{\|\mathbf{K}\mathbf{b}_2\|^2}{\sigma_d^2} + \frac{c\lambda_{g,1}\|\mathbf{H}\mathbf{b}_2\|^4}{\sigma_d^2 + \sigma_r^2c\lambda_{g,1}\|\mathbf{H}\mathbf{b}_2\|^2}\right) \qquad (49)$$

$$\text{s.t.} \quad \alpha\lambda_b + \frac{1-\alpha}{2}\|\mathbf{b}_2\|^2 \leq \frac{1+\alpha}{2}P_s \qquad (50)$$

$$c(\|\mathbf{H}\mathbf{b}_2\|^4 + \sigma_r^2\|\mathbf{H}\mathbf{b}_2\|^2) \leq \frac{2\alpha\xi}{1-\alpha}\lambda_{h,1}\lambda_b \qquad (51)$$

$$\lambda_b \leq P_m. \qquad (52)$$

If (52) is active, there is $\lambda_b = P_m$. In this case, we can further simplify the problem (49)-(52) as shown below.

Based on the discussions in Sections III-A and III-B, constraints (50) and (51) must be active at the optimal solution. Thus, by substituting $\lambda_b = P_m$ into (50) and (51), we have

$$\|\mathbf{b}_2\|^2 = P_\alpha - P_{m,\alpha} \tag{53}$$

$$c\|\mathbf{H}\mathbf{b}_2\|^2 = \frac{\lambda_{h,1}\xi P_{m,\alpha}}{\|\mathbf{H}\mathbf{b}_2\|^2 + \sigma_r^2} \tag{54}$$

where $P_{m,\alpha} = \frac{2\alpha}{1-\alpha}P_m$. Note that since both (50) and (52) are active, there is $P_m \le \frac{1+\alpha}{2\alpha}P_s$. By substituting (54) back into (49), we obtain the objective function as

$$\log_2\left(1 + \frac{1}{\sigma_d^2}\left(\|\mathbf{K}\mathbf{b}_2\|^2 + \frac{\sigma_d^2\|\mathbf{H}\mathbf{b}_2\|^2}{(1+\rho)\sigma_r^2 + \rho\|\mathbf{H}\mathbf{b}_2\|^2}\right)\right)$$

where $\rho = \frac{1}{\lambda P_{m,\alpha}}$. Similar to (34), we introduce $\|\mathbf{H}\mathbf{b}_2\|^2 \ge y$. In this way, the problem (49)-(52) is converted into the following problem

$$\max_{y,\mathbf{b}_2} \|\mathbf{K}\mathbf{b}_2\|^2 + \frac{\sigma_d^2 y}{(1+\rho)\sigma_r^2 + \rho y} \tag{55}$$

$$\text{s.t. } \|\mathbf{H}\mathbf{b}_2\|^2 \ge y \tag{56}$$

$$\|\mathbf{b}_2\|^2 = \zeta \tag{57}$$

where $\zeta = P_\alpha - P_{m,\alpha}$.

The Lagrangian function associated with the problem (55)-(57) is given by

$$L = -\|\mathbf{K}\mathbf{b}_2\|^2 - \frac{\sigma_d^2 y}{(1+\rho)\sigma_r^2 + \rho y} + \beta(y - \|\mathbf{H}\mathbf{b}_2\|^2)$$
$$+ \gamma(\|\mathbf{b}_2\|^2 - \zeta) \tag{58}$$

where $\beta \ge 0$ and γ are the Lagrange multipliers. From (58), the first-order optimality conditions can be written as

$$\frac{\partial L}{\partial \mathbf{b}_2} = -\mathbf{b}_2^H \mathbf{K}^H \mathbf{K} - \beta \mathbf{b}_2^H \mathbf{H}^H \mathbf{H} + \gamma \mathbf{b}_2^H = 0 \tag{59}$$

$$\frac{\partial L}{\partial y} = -\frac{(1+\rho)\sigma_r^2 \sigma_d^2}{((1+\rho)\sigma_r^2 + \rho y)^2} + \beta = 0. \tag{60}$$

From (57) and (59), it follows that

$$\mathbf{b}_2^* = \sqrt{\zeta}\mathbf{v}(\beta^*\mathbf{H}^H\mathbf{H} + \mathbf{K}^H\mathbf{K}). \tag{61}$$

Based on the discussion in Section III-B, the constraint (56) is active at the optimal solution. Thus, we obtain

$$y^* = \zeta\|\mathbf{H}\mathbf{v}(\beta^*)\|^2. \tag{62}$$

Therefore, the problem (55)-(57) is reduced to finding β^*, and this is equivalent to solving the following nonlinear equation, which is obtained by substituting (62) back into (60)

$$\beta - \frac{(1+\rho)\sigma_r^2\sigma_d^2}{((1+\rho)\sigma_r^2 + \rho\zeta\|\mathbf{H}\mathbf{v}(\beta)\|^2)^2} = 0. \tag{63}$$

As the left-hand side of (63) monotonically increases with β, (63) can be efficiently solved by the bisection method.

Based on the discussions above, we propose a two-step approach to solve the problem (49)-(52). In the first step, we apply Algorithm 2 to solve the problem (49)-(51) by omitting (52). Then, we check whether (52) is satisfied or not. If it is satisfied, then we adopt the obtained solution. If not, we solve the problem (49)-(52) via solving (63) in the second

---

Algorithm 3 Procedure of Solving the Problem (49)-(52).

Input: α, P_s, P_m, λ, σ_r^2, σ_d^2, $\mathbf{H}$, and $\mathbf{K}$.
Output: $\mathbf{b}_2^*$ and c^*.
1: Solve the problem (49)-(51) for $\mathbf{b}_2^*$ and c^* by applying Algorithm 2.
2: **if** $\lambda_b^* = \frac{(1-\alpha^*)c^*}{2\alpha^*\xi\lambda_{h,1}}\left(\|\mathbf{H}\mathbf{b}_2^*\|^4 + \sigma_r^2\|\mathbf{H}\mathbf{b}_2^*\|^2\right) \le P_m$ **then**
3:     Stop and return $\mathbf{b}_2^*$ and c^*.
4: **else**
5:     Solve (63) for β^*. Calculate $\mathbf{b}_2^*$ and c^* according to (61) and (54), respectively.
6: **end if**.

---

step. We refer this approach as Algorithm 3 and summarize it as follows.

REMARK 2: It can be seen from Algorithm 3 that only one nonlinear equation needs to be solved in the second step. Interestingly, for the problem (49)-(52), the generalized beamforming structure still holds for $\mathbf{b}_2$ in (61). Note that Algorithm 2 can be reused in solving the problem (49)-(52).

REMARK 3: When α approaches 1, $\|\mathbf{b}_2\|$ in (50) and $\|\mathbf{H}\mathbf{b}_2\|$ in (51) might increase to large value. To impose peak power constraints in this case, we have $\|\mathbf{b}_2\|^2 \le P_{m,2}$ and $c(\|\mathbf{H}\mathbf{b}_2\|^4 + \sigma_r^2\|\mathbf{H}\mathbf{b}_2\|^2) \le P_{m,3}$. If these two constraints are active, there must be

$$\|\mathbf{b}_2\|^2 = P_{m,2} \tag{64}$$

$$c\|\mathbf{H}\mathbf{b}_2\|^2 = \frac{P_{m,3}}{\|\mathbf{H}\mathbf{b}_2\|^2 + \sigma_r^2}. \tag{65}$$

Since (64) and (65) are similar to (53) and (54), the analysis in (55)-(63) can be applied in the transceiver design with peak power constraints when α approaches 1.

IV. SIMULATIONS

In this section, we study the performance of the proposed algorithm via numerical simulations. In the simulations, the three nodes are located in a line, where the distance between the source node and the destination node is 20 meters, and the distance between the source node and the relay node is $10d$ meters, where the value of $0 < d < 2$ is normalized over a distance of 10 meters. Therefore, the relay-destination distance is $10(2-d)$. The path loss exponent is set to 3. We set the power harvesting efficiency $\xi = 0.8$. The noise power at the relay and the destination nodes is fixed as $\sigma_r^2 = \sigma_d^2 = -50$dBm. For all simulation examples, we choose $N_s = N_r = N_d = N$, and the results are averaged over 1000 independent channel realizations.

A. Example 1: Rate versus the Nominal Source Node Power

In the first example, we set $d = 1$ and compare the performance of the proposed algorithm (Algorithm 1, where Algorithm 2 is applied to solve the problem (29)-(30)) with the fixed α algorithm (Algorithm 2 only with $\alpha = 0.3$, $\alpha = 0.5$, and $\alpha = 0.8$, respectively). The achievable rates of the proposed algorithm and the fixed α approach versus the nominal power P_s for $N = 3$ and $N = 5$ are shown in Fig. 3 and Fig. 4, respectively. From Figs. 3 and 4, we
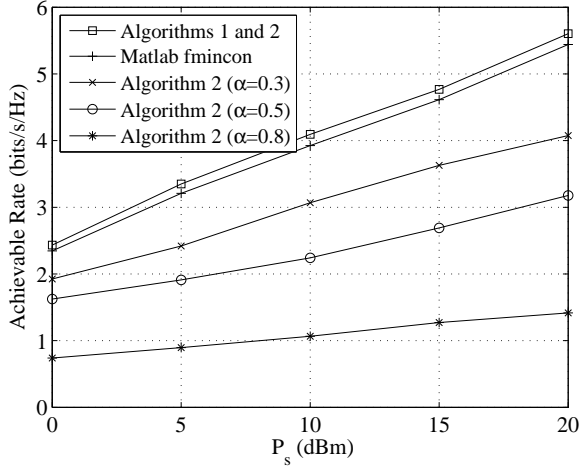
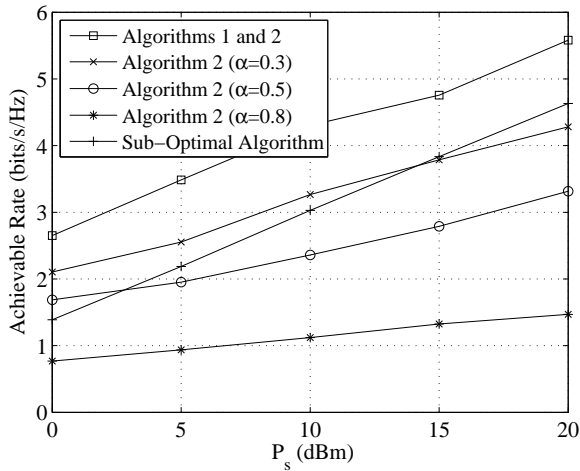Fig. 3.   Example 1: Rate versus P_s, $d = 1$, $N = 3$.

Fig. 4.   Example 1: Rate versus P_s, $d = 1$, $N = 5$.

observe that the proposed algorithm performs better than the fixed α scheme. This is because α is optimized in our proposed algorithm so that a higher rate is obtained. Moreover, it can be seen that the achievable rate with $N = 5$ in Fig. 4 is higher than that of $N = 3$ in Fig. 3. This is because the harvested power is increased with a larger number of antennas at the relay node. As a benchmark, we solve the problem (18)-(20) using the Matlab fmincon nonlinear programming toolbox. In particular, for each channel realization, 10 random initializations are attempted and the one yields the largest system rate is chosen. It can be seen from Fig. 3 that the proposed algorithm achieves a higher rate than that using the fmincon toolbox.

The performance comparison between the proposed algorithm and a sub-optimal scheme is also shown in Fig. 4. The sub-optimal approach is obtained by neglecting the direct link $\mathbf{K}$, i.e., we choose $\mathbf{b}_2^* = \sqrt{\eta^*}\mathbf{v}(\mathbf{H}^H\mathbf{H})$ in (42). Thus, we only need to solve η in (46). As expected, we can see from Fig. 4 that the performance of the proposed algorithm is better than the sub-optimal approach due to the consideration of the direct
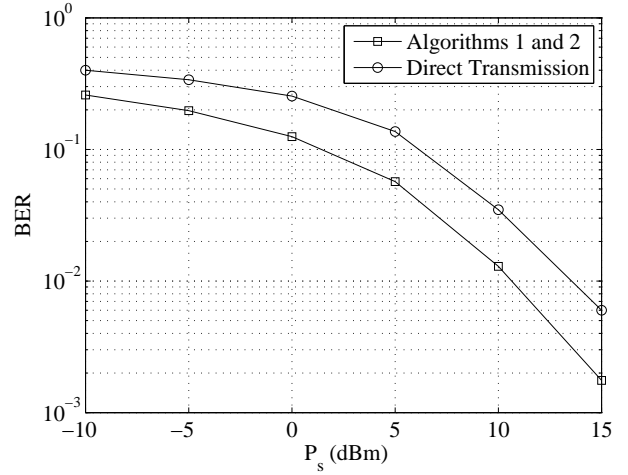

Fig. 5.   Example 2: BER versus P_s, $d = 0.5$, $N = 3$.

link channel $\mathbf{K}$.

B. Example 2: BER Performance

In this example, we study the BER performance of the proposed system with $d = 0.5$ and $N = 3$. Fig. 5 shows the raw (uncoded) BER comparison of the proposed system with the direct transmission system without using any relay node. The transmitted signals are modulated by QPSK constellations. It can be seen from Fig. 5 that the proposed system has a smaller BER than the direct transmission system. This is mainly achieved by the spatial diversity provided by the source-relay-destination link.

C. Example 3: Time Switching Factor versus the Nominal Source Node Power

To further interpret the performance gain of the proposed algorithm in the first example, we plot the optimal time switching factor α calculated by the proposed algorithm in the third example. In this example, we set $d = 1$. Fig. 6 shows the optimal α versus the nominal power P_s with $N = 3$ and $N = 5$. It can be seen from Fig. 6 that for the proposed algorithm, the optimal α monotonically decreases as the nominal power P_s increases. In particular, the optimal α becomes very small when P_s is above 12dBm. The reason is that when P_s is large enough, λ_b (the power level at the source node at the first interval) obtained by the proposed algorithm increases. Thus, even though α is small, the energy $\alpha\lambda_{h,1}\lambda_b$ harvested by the relay node is sufficient to forward the signal to the destination node. Therefore, more time can be allocated for information transmission so that a higher data rate can be achieved at large P_s. We also observe from Fig. 6 that the optimal α is slightly smaller for $N = 5$ than that for $N = 3$. This is because with a larger number of antennas, more power can be harvested at the relay node per unit time, and thus, a smaller α is sufficient for the relay node to harvest the energy required for forwarding the information signals.
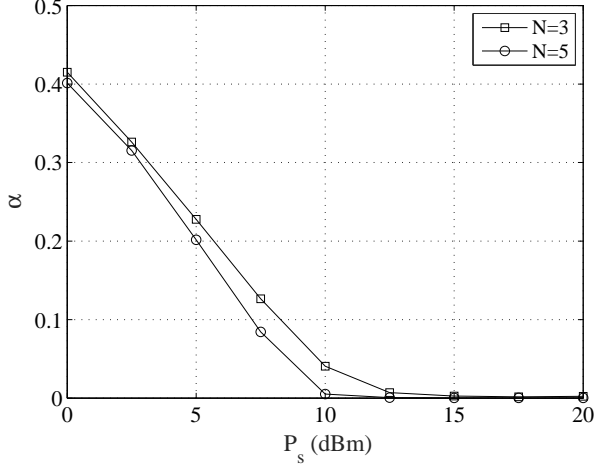
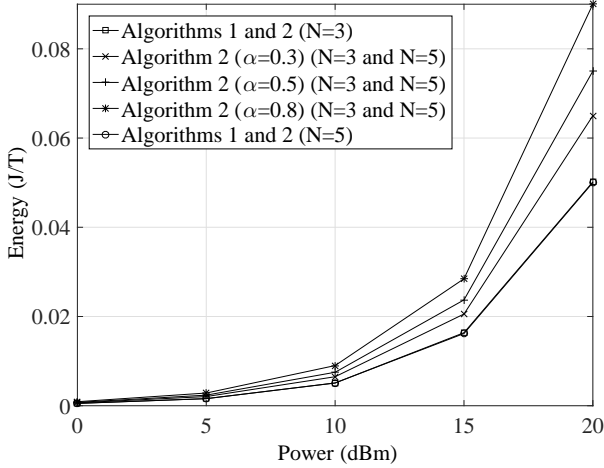Fig. 6. Example 3: Optimal α versus P_s with $d = 1$.

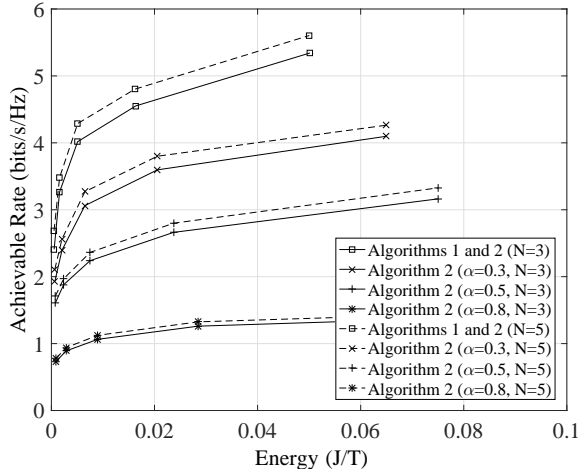Fig. 7. Example 4: Energy consumption versus P_s, $d = 1$.
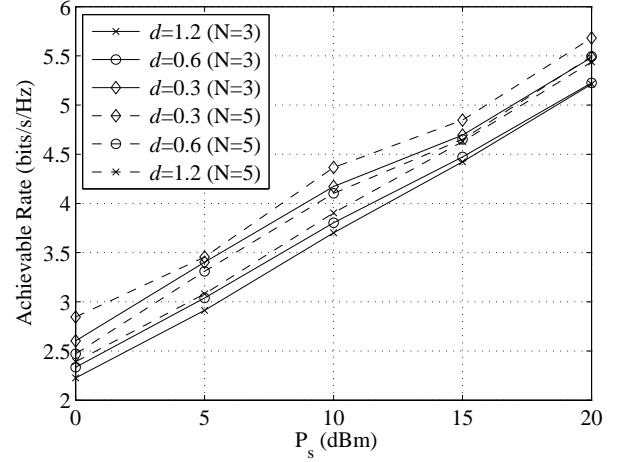

Fig. 8. Example 4: Rate versus energy, $d = 1$.

Fig. 9. Example 5: Rate versus P_s at various d.

D. Example 4: Rate and Energy Consumption Trade-off Comparison

In this example, we fix $d = 1$ and study the energy consumption $P_s(1 + \alpha)/2$ and rate-energy trade-off of the proposed algorithm. We first plot the energy consumption versus P_s in Fig. 7. Then, we plot the achievable rate versus energy in Fig. 8. As shown in Fig. 7, the energy cost for the proposed algorithm is lower than fixed α schemes. The better rate-energy trade-off achieved by the proposed algorithm is demonstrated in Fig. 8. This indicates that the proposed algorithm achieves a higher rate with a less energy consumption through optimizing α.

Interestingly, it can be seen from Fig. 7 that the energy consumption for $N = 3$ and $N = 5$ is almost the same. This can be explained based on Fig. 6. As the optimal α for $N = 3$ and $N = 5$ is similar at high P_s, the energy consumption of two systems is also similar. However, the rate achieved by $N = 5$ is higher than that by $N = 3$ as shown in Fig. 8. This implies that the system energy efficiency can be further improved by increasing the number of antennas.

E. Example 5: Achievable Rate at Various d

In this example, we study the achievable rate at various d. First, we plot the rate versus P_s for the proposed algorithm with different d in Fig. 9. Then we compare the proposed algorithm with the fixed α schemes by plotting the rate versus d in Fig. 10. From Figs. 9 and 10, we observe that the achievable rate decreases as d increases, and the proposed method performs better than any fixed α algorithms. As expected, the rate increases when N is larger.

F. Example 6: Practical Peak Power Constraint

In the last example, we set $d = 1$, $N = 5$, and test the proposed algorithm with a practical peak power constraint. We plot the rate versus P_s for the system with only the energy-constraint (Algorithms 1 and 2) and the system considering the peak power constraint (52) (Algorithms 1 and 3) in Fig. 11. We set $P_m = \kappa P_s$ and choose $\kappa = 1$, $\kappa = 2$, and $\kappa = 10$.
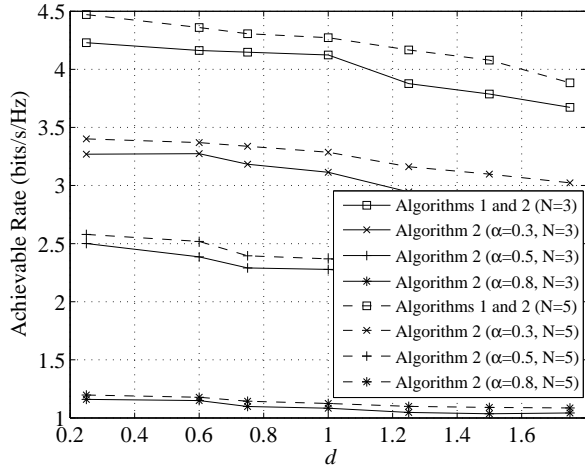
Fig. 10. Example 5: Rate versus d, $P_s = 10$dBm.

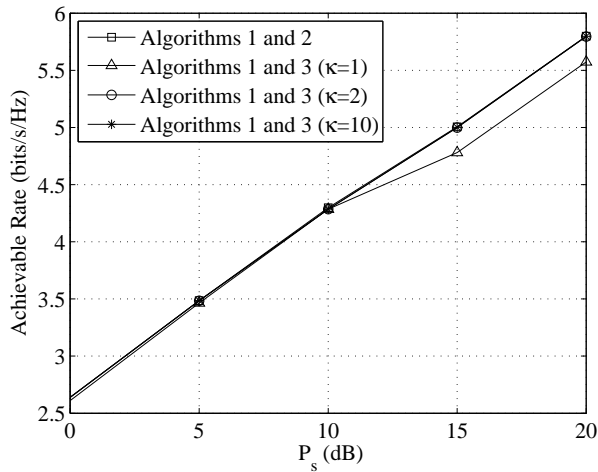Fig. 12. Example 6: Optimal α versus P_s at various peak power constraints, $d = 1$, $N = 5$.

Fig. 11. Example 6: Rate versus P_s at various peak power constraints, $d = 1$, $N = 5$.

We observe from Fig. 11 that as expected, the rate decreases slightly with κ. Interestingly, the performance of the algorithm with the peak power constraint converges to the one with only the energy constraint as κ increases.

Next, we plot the optimal α versus P_s for the two systems with various κ in Fig. 12. It can be seen from Fig. 12 that for the system with peak power constraint, the optimal time switching factor α decreases as P_m increases, and it converges to the one with only the energy constraint. It reveals the same relationship between the energy constraint and peak power constraint as that in Fig. 11. The reason is that with the same amount of energy the time required for energy transfer decreases as the allowable power increases, and longer time can be used for transmitting information signals so that the rate performance can be improved.

V. CONCLUSIONS

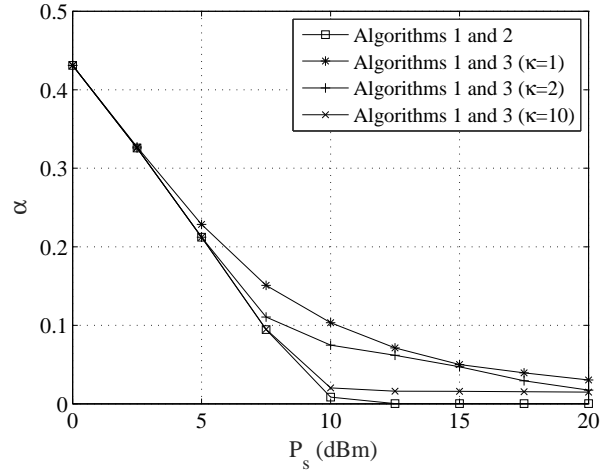A new TS protocol for WPC in two-hop AF MIMO relay networks with direct link has been developed in this paper. The joint optimization of the source and relay precoding matrices and the TS factor is studied to maximize the source-destination rate subjecting to an energy constraint at the source node and an EH constraint at the relay node. The optimal structure of the source and relay precoding matrices has been derived, which reduces the original problem to a simpler problem. In particular, we show that the optimal source precoding vector for the information transfer has a generalized beamforming structure. A two-step method has been developed to solve this problem. The optimal TS factor has been obtained by the golden section search method. For a given TS factor, the remaining variables are optimized via solving two nonlinear equations by exploring the structure of the problem. To limit the power of energy transfer at the source node, a practical peak power constraint is considered. A two-step approach is proposed by checking the activeness of this constraint. Numerical studies show that the proposed algorithm performs better than approaches without optimizing the TS factor. It is shown that the rate achieved by systems with peak power constraint approaches that of the system with only energy constraint when the value of the peak power is high.

APPENDIX A
PROOF OF THEOREM 1

The following results from [14] is needed to prove Theorem 1.

LEMMA 1 [14]: The optimal $\mathbf{F}$ as the solution to the following relay precoding matrix optimization problem

$$\max_{\mathbf{F}} \ 1 + \sigma_d^{-2}\mathbf{b}_2^H\mathbf{K}^H\mathbf{K}\mathbf{b}_2 + \mathbf{b}_2^H\mathbf{H}^H\mathbf{F}^H\mathbf{G}^H$$

$$\times (\sigma_r^2\mathbf{G}\mathbf{F}\mathbf{F}^H\mathbf{G}^H + \sigma_d^2\mathbf{I}_{N_d})^{-1}\mathbf{G}\mathbf{F}\mathbf{H}\mathbf{b}_2 \quad (66)$$

$$\text{s.t. } \text{tr}(\mathbf{F}(\mathbf{H}\mathbf{b}_2\mathbf{b}_2^H\mathbf{H}^H + \sigma_r^2\mathbf{I}_{N_r})\mathbf{F}^H) \leq P_r \quad (67)$$

is given by

$$\mathbf{F}^* = \sqrt{\frac{P_r}{\|\mathbf{H}\mathbf{b}_2\|^4 + \sigma_r^2\|\mathbf{H}\mathbf{b}_2\|^2}} \mathbf{v}_{g,1}\mathbf{b}_2^H\mathbf{H}^H \quad (68)$$

where $\mathbf{v}_{g,1}$ is given by (21).

Now we start to prove Theorem 1. First we prove the optimal structure of $\mathbf{B}_1$. It can be seen from (18)-(20) that $\mathbf{B}_1$ does not appear explicitly in the objective function (18), and it affects (18) through changing the feasible region of the problem specified by the constraints (19) and (20). Therefore, in order to maximize the feasible region, for *any* $\mathrm{tr}(\mathbf{B}_1\mathbf{B}_1^H)$, we should maximize $\mathrm{tr}(\mathbf{H}\mathbf{B}_1\mathbf{B}_1^H\mathbf{H}^H)$, which can be written as the following optimization problem

$$\max_{\mathbf{B}_1} \ \mathrm{tr}(\mathbf{H}\mathbf{B}_1\mathbf{B}_1^H\mathbf{H}^H) \tag{69}$$

$$\text{s.t. } \mathrm{tr}(\mathbf{B}_1\mathbf{B}_1^H) = \lambda_b \tag{70}$$

where λ_b is a positive scalar. From Proposition 2.1 of [8], the solution to the problem (69)-(70) satisfies $\mathbf{B}_1^*\mathbf{B}_1^{*H} = \lambda_b\mathbf{v}_{h,1}\mathbf{v}_{h,1}^H$. Therefore, we prove

$$\mathbf{B}_1^* = \lambda_b^{\frac{1}{2}}\mathbf{v}_{h,1}. \tag{71}$$

By substituting (71) back into the problem (18)-(20), we have the problem of

$$\max_{0<\alpha<1,\lambda_b,\mathbf{b}_2,\mathbf{F}} \ \mathrm{R}(\alpha,\mathbf{b}_2,\mathbf{F})$$

$$\text{s.t. } \mathrm{tr}(\mathbf{b}_2\mathbf{b}_2^H) \le \frac{2}{1-\alpha}\left(\frac{1+\alpha}{2}P_s - \alpha\lambda_b\right)$$

$$\mathrm{tr}(\mathbf{F}(\mathbf{H}\mathbf{b}_2\mathbf{b}_2^H\mathbf{H}^H+\sigma_r^2\mathbf{I}_{N_r})\mathbf{F}^H) \le \frac{2\alpha\xi}{1-\alpha}\lambda_b\lambda_{h,1}.$$

For a given $\mathbf{b}_2$, the relay precoding matrix $\mathbf{F}$ is optimized by solving the following problem

$$\max_{0<\alpha<1,\lambda_b,\mathbf{F}} \ \mathrm{R}(\alpha,\mathbf{F}) \tag{72}$$

$$\text{s.t. } \mathrm{tr}(\mathbf{F}(\mathbf{H}\mathbf{b}_2\mathbf{b}_2^H\mathbf{H}^H+\sigma_r^2\mathbf{I}_{N_r})\mathbf{F}^H) \le \frac{2\alpha\xi}{1-\alpha}\lambda_b\lambda_{h,1} \tag{73}$$

It can be seen that for *any* given α and λ_b, the problem (72)-(73) is in the same form as the problem (66)-(67). Therefore, $\mathbf{F}^*$ in (22) is proven based on (68) in Lemma 2. $\qquad\square$

APPENDIX B
PROOF OF PROPOSITION 1

By introducing $\mathbf{\Phi} = \mathbf{b}_2\mathbf{b}_2^H$ and neglecting the constraint of $\mathrm{rank}(\mathbf{\Phi}) = 1$, where $\mathrm{rank}(\cdot)$ denotes the matrix rank, the problem (35)-(37) can be relaxed to the following problem

$$\max_{x,y,\mathbf{\Phi}\ge 0} \ \mathrm{tr}(\mathbf{K}\mathbf{\Phi}\mathbf{K}^H) + \frac{\sigma_d^2 xy}{\sigma_r^2 x + y + \sigma_r^2} \tag{74}$$

$$\text{s.t. } \mathrm{tr}(\mathbf{H}\mathbf{\Phi}\mathbf{H}^H) \ge y \tag{75}$$

$$\mathrm{tr}(\mathbf{\Phi}) \le P_\alpha - x/\lambda. \tag{76}$$

The problem (74)-(76) is a convex optimization problem, as it can be verified that $\frac{\sigma_d^2 xy}{\sigma_r^2 x+y+\sigma_r^2}$ is a jointly concave function of (x,y) based on its Hessian matrix. Therefore, this problem admits strong duality [34]. Interestingly, as the problem (74)-(76) is a semidefinite programming (SDP) problem with two linear constraints, the approach in [35] can be used to obtain a rank-1 optimal solution of this problem. This indicates that the problem (35)-(37) and the problem (74)-(76) share the same optimal solution. Moreover, it can be shown that the dual problem of (35)-(37) and the dual problem of (74)-(76) are identical. Therefore, the problem (35)-(37) also admits strong duality. $\qquad\square$

APPENDIX C
THE JACOBIAN MATRIX OF (47)

For the simplicity of notations, we denote $f_1(\beta,\eta)$, $f_2(\beta,\eta)$, and $\Delta(\beta,\eta)$ as f_1, f_2, and Δ, respectively. We have

$$J = \begin{bmatrix} \frac{\partial f_1}{\partial \beta} & \frac{\partial f_1}{\partial \eta} \\ \frac{\partial f_2}{\partial \beta} & \frac{\partial f_2}{\partial \eta} \end{bmatrix}$$

where

$$\frac{\partial f_1}{\partial \beta} = \Delta + \beta\frac{\partial \Delta}{\partial \beta}$$

$$\frac{\partial f_1}{\partial \eta} = \beta\frac{\partial \Delta}{\partial \eta} + 2\sigma_r^2\sigma_d^2\lambda^2(P_\alpha - \eta) + \lambda\sigma_r^2\sigma_d^2$$

$$\frac{\partial f_2}{\partial \beta} = \frac{\mathrm{d}e(\beta)}{\mathrm{d}\beta}\Delta + e(\beta)\frac{\partial \Delta}{\partial \beta}$$

$$- \sigma_d^2\lambda\eta\frac{\mathrm{d}\|\mathbf{H}\mathbf{v}(\beta)\|^2}{\mathrm{d}\beta}(2\eta\|\mathbf{H}\mathbf{v}(\beta)\|^2 + \sigma_r^2)$$

$$\frac{\partial f_2}{\partial \eta} = e(\beta)\frac{\partial \Delta}{\partial \eta} - \sigma_d^2\lambda\|\mathbf{H}\mathbf{v}(\beta)\|^2(2\eta\|\mathbf{H}\mathbf{v}(\beta)\|^2 + \sigma_r^2)$$

and

$$\frac{\partial \Delta}{\partial \beta} = 2\sqrt{\Delta}\eta\frac{\mathrm{d}\|\mathbf{H}\mathbf{v}(\beta)\|^2}{\mathrm{d}\beta}$$

$$\frac{\partial \Delta}{\partial \eta} = 2\sqrt{\Delta}(\|\mathbf{H}\mathbf{v}(\beta)\|^2 - \sigma_r^2\lambda)$$

$$\frac{\mathrm{d}e(\beta)}{\mathrm{d}\beta} = \mathbf{v}^H(\beta)\mathbf{H}^H\mathbf{H}\mathbf{v}(\beta)$$

$$\frac{\mathrm{d}\|\mathbf{H}\mathbf{v}(\beta)\|^2}{\mathrm{d}\beta} = \mathbf{v}^H(\beta)\mathbf{H}^H\mathbf{H}\left(e(\beta)\mathbf{I}_{N_s} - \beta\mathbf{H}^H\mathbf{H}\right.$$

$$\left. -\mathbf{K}^H\mathbf{K}\right)^{-1}\mathbf{H}^H\mathbf{H}\mathbf{v}(\beta).$$

Here, we have used the results on the derivatives of matrix eigenvalues and eigenvectors in [36].

ACKNOWLEDGEMENT

REFERENCES

[1] L. R. Varshney, "Transporting information and energy simultaneously," in *Proc. IEEE Int. Symp. Inf. Theory (ISIT)*, Toronto, Canada, July 6-11, 2008, pp. 1612-1616.

[2] Z. Ding, C. Zhong, D. W. K. Ng, M. Peng, H. A. Suraweera, R. Schober, and H. V. Poor, "Applications of smart antenna technologies in simultaneous wireless information and power transfer," *IEEE Commun. Mag.*, vol. 53, pp. 86-93, Apr. 2015.

[3] K. Xiong, P. Fan, C. Zhang, and K. B. Letaief, "Wireless information and energy transfer for two-hop non-regenerative MIMO-OFDM relay networks," *IEEE J. Select. Areas Commun.*, vol. 33, pp. 1595-1611, Aug. 2015.

[4] W. K. G. Seah, Z. A. Eu, and H. P. Tan, "Wireless sensor networks powered by ambient energy harvesting (WSN-HEAP) – Survey and challenges," in *Proc. Wireless VITAE*, May 2009, pp. 15.

[5] C. Huang, R. Zhang, and S. Cui, "Throughput maximization for the Gaussian relay channel with energy harvesting constraints," *IEEE J. Select. Areas Commun.*, vol. 31, pp. 1469-1479, Aug. 2013.

[6] D. T. Hoang, D. Niyato, P. Wang, and D. I. Kim, "Opportunistic channel access and RF energy harvesting in cognitive radio networks," *IEEE J. Select. Areas Commun.*, vol. 32, pp. 2039-2052, Nov. 2014.

[7] X. Zhou, R. Zhang, and C. K. Ho, "Wireless information and power transfer: Architecture design and rate-engergy trade-off," *IEEE Trans. Commun.,* vol. 61, pp. 4754-4767, Nov. 2013.

[8] R. Zhang and C. K. Ho, "MIMO broadcasting for simultaneous wireless information and power transfer," *IEEE Trans. Wireless Commun.*, vol. 12, pp. 1989-2001, May 2013.

[9] B. Li, C. Z. Wu, H. H. Dam, A. Cantoni, and K. L. Teo, "A parallel low complexity zero-forcing beamformer design for multiuser MIMO systems via a regularized dual decomposition method," *IEEE Trans. Signal Process.*, vol. 63, pp. 4179-4190, Aug. 2015.

[10] B. Li, Y. Rong, J. Sun, and K. L. Teo, "A distributionally robust linear receiver design for multi-access space-time block coded MIMO systems," *IEEE Trans. Wireless Commun.*, vol. 16, pp. 464-474, Jan. 2017.

[11] Q. Shi, L. Liu, W. Xu, and R. Zhang, "Joint transmit beamforming and receieve power splitting for MISO SWIPT," *IEEE Trans. Wireless Commun.*, vol. 13, pp. 3269-3280, June 2014.

[12] X. Tang and Y. Hua, "Optimal design of non-regenerative MIMO wireless relays," *IEEE Trans. Wireless Commun.*, vol. 6, no. 4, pp. 1398-1407, Apr. 2007.

[13] Y. Rong, "Optimal joint source and relay beamforming for MIMO relays with direct link," *IEEE Commun. Lett.*, vol. 14, pp 390-392, May 2010.

[14] Y. Rong and F. Gao, "Optimal beamforming for non-regenerative MIMO relays with direct link," *IEEE Commun. Lett.*, vol. 13, pp. 926-928, Dec. 2009.

[15] M. R. A. Khandaker and Y. Rong, "Joint transceiver optimization for multiuser MIMO relay communication systems," *IEEE Trans. Signal Process.*, vol. 60, pp. 5997-5986, Nov. 2012.

[16] Z. He, J. Zhang, W. Liu, and Y. Rong, "New results on transceiver design for two-hop amplify-and-forward MIMO relay systems with direct link," *IEEE Trans. Signal Process.*, vol. 64, pp. 5232-5241, Oct. 2016.

[17] A. A. Nasir, X. Zhou, S. Durrani, and R. A. Kennedy, "Relaying protocols for wireless energy harvesting and information processing," *IEEE Trans. Wireless Commun.*, vol. 12, pp. 3622-3636, July 2013.

[18] Y. Zeng and R. Zhang, "Full-duplex wireless-powered relay with self-energy recycling," *IEEE Wireless Commun. Lett.*, vol. 4, pp. 201-204, Apr. 2015.

[19] Z. Ding, S. M. Perlaza, I. Esnaola, and H. V. Poor, "Power allocation strategies in energy harvesting wireless cooperative networks," *IEEE Trans. Wireless Commun.*, vol. 13, pp. 846-860, Feb. 2014.

[20] Z. Ding, I. Esnaola, B. Sharif, and H. V. Poor, "Wireless information and power transfer in cooperative networks with spatially random relays," *IEEE Trans. Wireless Commun.*, vol. 13, pp. 4400-4453, Aug. 2014.

[21] H. Chen, Y. Li, Y. Jiang, Y. Ma, and B. Vucetic, "Distributed power splitting for SWIPT in relay interference channnles using game theory," *IEEE Trans. Wireless Commun.*, vol. 14, pp. 410-420, Jan. 2015.

[22] X. Di, K. Xiong, P. Fan, and H.-C. Yang, "Simultaneous wireless information and power transfer in cooperative relay networks with rateless codes," *IEEE Trans. Veh. Technol.*, vol. 66, pp. 2981-2996, Apr. 2017.

[23] B. Fang, W. Zhong, S. Jin, Z. Qian, and W. Shao, "Game-theoretic precoding for SWIPT in the DF-based MIMO relay networks," *IEEE Trans. Veh. Technol.*, vol. 65, pp. 6940-6948, Sep. 2016.

[24] J. Huang, H. Chen, Y. Jiang, J. Meng, A. Xu, X. Guo, and B. Chen, "Precoder design for MIMO decode-and-forward relay channels with energy harvesting constraint," in *Proc. IEEE Conf. Industrial Electronics Applications*, Hefei, China, June 5-7, 2016, pp. 368-372.

[25] B. K. Chalise, Y. D. Zhang, and M. G. Amin, "Energy harvesting in an OSTBC based non-regenerative MIMO relay system," in *Proc. IEEE ICASSP*, Mar. 2012, pp. 3201-3204.

[26] B. K. Chalise, W. K. Ma, Y. D. Zhang, H. Suraweera, and M. G. Amin, "Optimum performance boundaries of OSTBC based AF-MIMO relay system with energy harvesting receiver," *IEEE Trans. Signal Process.*, vol. 61, pp. 4199-4213, Sep. 2013.

[27] K. Xiong, P. Fan, H. C. Yang, and K. B. Letaief, "Optimal cooperative beamforming design for MIMO decode-and-forward relay channels," *IEEE Trans. Signal Process.*, vol. 62, pp. 1476-1489, Mar. 2014.

[28] R. Zhang, Y. C. Liang, C. C. Chai, and S. Cui, "Optimal beamforming for two-way multi-antenna relay channel with analogue network coding," *IEEE J. Select. Areas Commun.*, vol. 27, pp. 699-712, June 2009.

[29] Y. Zeng, B. Clerckx, and R. Zhang, "Communications and signals design for wireless power transmission," *IEEE Trans. Commun.*, vol. 65, pp. 2264-2290, May, 2017.

[30] E. Boshkovska, D. W. K. Ng, N. Zlatanov, and R. Schober, "Practical non-linear energy harvesting model and resource allocation for SWIPT systems," *IEEE Commun. Lett.*, vol. 19, pp. 2082-2085, Dec. 2015.

[31] K. Xiong, B. Wang, and K. J. R. Liu, "Rate-energy region of SWIPT for MIMO broadcasting under nonlinear energy harvesting model," *IEEE Trans. Wireless Commun.*, vol. 16, pp. 5147-5161, Aug. 2017.

[32] R. Jiang, K. Xiong, P. Fan, Y. Zhang, and Z. Zhong, "Optimal design of SWIPT systems with multiple heterogeneous users under non-linear energy harvesting model," *IEEE Access*, vol. 5, pp. 11479-11489, Jul. 2017.

[33] A. Antoniou and W.-S. Lu, *Practical Optimization: Algorithms and Engineering Applications*. Spring Street, NY: Springer Science+Business Media, LCC, 2007.

[34] S. Boyd and L. Vandenberghe, *Convex Optimization*. Cambridge, U. K.: Cambridge University Press, 2004.

[35] W. Ai, Y. Huang, and S. Zhang, "New results on Hermitian matrix rank-one decomposition," *Math. Programm.*, vol. 128, pp. 253-283, Aug. 2009.

[36] D. V. Murthy and R. T. Haftka, "Derivatives of eigenvalues and eigenvectors of a general complex matrix," *Int. J. Numer. Meth. Eng.*, vol. 26, pp. 293-311, Feb. 1988.

PLACE PHOTO HERE

Bin Li received the Bachelor degree in automation and the Master degree in control science and engineering from Harbin Institute of Technology, China, in 2005 and 2008, respectively, and Ph.D. degree in mathematics and statistics from Curtin University, Australia, in 2011. From 2012 - 2014, he was a Research Associate with the School of Electrical, Electronic and Computer Engineering, the University of Western Australia, Australia. From 2014 to 2017, he was a Research Fellow with the Department of Mathematics and Statistics, Curtin University, Australia. Currently, he is a Professor with the School of Electrical Engineering and Information, Sichuan University. His research interests include signal processing, wireless communications, optimization and optimal control.

PLACE PHOTO HERE

Yue Rong (S'03-M'06-SM'11) received the Ph.D. degree (summa cum laude) in electrical engineering from the Darmstadt University of Technology, Darmstadt, Germany, in 2005.

He was a Post-Doctoral Researcher with the Department of Electrical Engineering, University of California, Riverside, from February 2006 to November 2007. Since December 2007, he has been with the Department of Electrical and Computer Engineering, Curtin University, Bentley, Australia, where he is currently a Professor. His research interests include signal processing for communications, wireless communications, underwater acoustic communications, applications of linear algebra and optimization methods, and statistical and array signal processing. He has published over 150 journal and conference papers in these areas.

Dr. Rong was a recipient of the Best Paper Award at the 2011 International Conference on Wireless Communications and Signal Processing, the Best Paper Award at the 2010 Asia-Pacific Conference on Communications, and the Young Researcher of the Year Award of the Faculty of Science and Engineering at Curtin University in 2010. He is an Associate Editor of the IEEE TRANSACTIONS ON SIGNAL PROCESSING. He was an Editor of the IEEE WIRELESS COMMUNICATIONS LETTERS from 2012 to 2014, a Guest Editor of the IEEE JOURNAL ON SELECTED AREAS IN COMMUNICATIONS special issue on theories and methods for advanced wireless relays, and was a TPC Member for the IEEE ICC, WCSP, IWCMC, EUSIPCO, and ChinaCom.